Laser-Induced Formation, Fragmentation, Coalescence, and Delayed Ionization of the $C_{59}N$ Heterofullerene

Nigel L. Clipston,[†] Tracy Brown,[†] Yury Y. Vasil′ev,[†] Mark P. Barrow,[†] Rainer Herzschuh,[‡] Uwe Reuther,[§] Andreas Hirsch,[§] and Thomas Drewello*[,†]

Department of Chemistry, University of Warwick, Coventry CV4 7AL, England, U.K., Fachbereich Chemie, Universität Leipzig, Linnéstrasse 3, D-04103 Leipzig, Germany, and Institut für Organische Chemie, Universität Erlangen, Henkestrasse 42, D-91054 Erlangen

Received: May 18, 2000; In Final Form: July 25, 2000

The formation of the nitrogen heterofullerene, $C_{59}N$, following the ablation of a variety of fullerene derivatives, all of which possess organic ligands bound to the carbon cage through a nitrogen atom, has been investigated utilizing laser desorption/ionization mass spectrometry. Investigating the formation of cationic and anionic $C_{59}N^{+/-}$, this approach is found to be a new and very efficient way to implement the initially exohedral nitrogen atom into the carbon cage. The laser-induced heterofullerene formation is discussed in terms of the structure and the charge state dependency of the target material. In further experiments, the coalescence reactivity, leading toward the formation of larger clusters has been examined following laser ablation of thin films of the $(C_{59}N)_2$ dimer. Coalescence leads to two major reaction products, consisting of larger $C_{n-1}N^+$ clusters which retain the nitrogen atom networked into a larger carbon cage and pure C_n^+ (n = even) carbon clusters. The $C_{n-1}N^+$ cluster formation is accompanied by abundant metastable transitions caused by the loss of CN and the resulting implications for the coalescence mechanism are discussed. Finally, evidence is presented for the delayed electron emission of $C_{59}N^{\bullet}$. The observation of delayed ionization of heterofullerenes is unprecedented, revealing a similar resistance toward fragmentation as in the case of their all-carbon fullerene analogues.

Introduction

The modification of the all-carbon fullerene cage by implementing one (or more) non-carbon atom(s) into the cage structure represents a promising approach to alter the material properties of pure fullerenes. Besides the perturbations on stability and geometrical features, the changes induced to the electronic character and chemical reactivity are of prime interest when considering potential applications of these materials. Heterofullerenes of this kind, also referred to as doped fullerenes, are accessible by a variety of methods, most of which are based on established techniques for the production of fullerenes which are modified to allow for the presence of the dopant to take part in the cage formation. Methods such as laser ablation,[1−4] carbon arcing,[5,6] and evaporation by inductive heating[7] have been successfully applied to produce heterofullerenes of the general type $C_{60-n}X_n$ with the doping atom predominantly given by X = B,[1,3,6] Si,[3,4] N,[2,5] and P.[7] Essentially the same structural principle holds also true for so-called "networked" metallofullerenes,[8−10] in which X represents a heavier metal atom. Although the methods mentioned above allow the preparation of macroscopic quantities of the respective heterofullerene, the vast majority are fairly unselective toward the production of only one major product and hence require laborious separation procedures to purify and accumulate the desired heterofullerene. A notable exception, however, exists in the case of nitrogen-containing heterofullerenes. The dimers of the azafullerenyl radical $C_{59}N^{\bullet}$ and its higher homologue $C_{69}N^{\bullet}$ are produced in macroscopic quantities as major products by organic synthesis.[11,12] The synthetic precursors include intact or partly cage-opened fullerenes, both of which contain organic ligands which are attached via a nitrogen atom. The initial inspirations for the synthetic routes that were developed to produce $(C_{59}N)_2$ derived from the detection of $C_{59}N^+$ by fast atom bombardment (FAB) or liquid secondary ion mass spectrometry (LSIMS).[11,13]

The present investigation focuses on the laser-induced gas-phase generation of nitrogen-containing heterofullerenes. In particular, a new approach for the formation of the $C_{59}N^+$ cation, the isoelectronic counterpart of neutral C_{60}, is presented by applying laser ablation of solid films of structurally related, exohedrally modified fullerenes incorporating nitrogen-attached organic ligands. The formation mechanism of this heterofullerene is studied by ablation of composite targets of pure and derivatized fullerenes, as well as by examining the generation of the anionic analogue, $C_{59}N^-$.

An interesting phenomenon connected with the laser ablation of pure and derivatized fullerenes consists of their ability to undergo fusion reactions to form larger entities.[14] In these so-called coalescence reactions, energized species react with each other in the high particle density of the fast expanding plume which accompanies the desorption event. The analysis of the product distribution derived from different fullerene-based materials activated at varying laser fluences has revealed important insight into both the reacting particles and the structural characteristics of the larger clusters produced in these reactions.[15−18] Considering the chemical changes induced by the networked heteroatom, the coalescence reactivity of aza-

* Corresponding author. Fax: +44-2476-524112. E-mail: t.drewello@warwick.ac.uk.
[†] Department of Chemistry.
[‡] Fachbereich Chemie.
[§] Institut für Organische Chemie.

10.1021/jp001837j CCC: $19.00
Published on Web 09/20/2000

heterofullerenes represents a particularly interesting case to be examined. In particular, the question of the degree to which the nitrogen atoms will be retained in the larger fusion products is of prime mechanistic importance.

Another most remarkable fullerene property is the ability to undergo delayed electron emission.[19,20] This process is commonly ascribed either to thermionic emission of electrons or to electron emission from long-lived, electronically excited states (for a recent reference, see[21] and references therein). The process affords a sufficiently high dissociation energy of the neutral compared to its ionization energy, so that ionization can dominate fragmentation as a relaxation channel for the "hot", energized species. As a consequence, the observation that delayed ionization occurs can be regarded as a statement on the stability of the species under investigation. Besides pure fullerenes, the only derivatized fullerenes that are so far found to undergo delayed ionization are endohedral metallofullerenes.[22] In the case of exohedrally modified fullerenes, fragmentation prevails without the occurrence of delayed ionization. It is therefore an intriguing question if heterofullerenes possess a sufficiently high stability to undergo delayed electron emission. This investigation reports the observation of delayed ionization of the monomeric azaheterofullerene $C_{59}N^{\cdot}$ after laser excitation.

Experimental Section

Laser desorption/ionization has been accomplished by the use of a nitrogen laser applying 337 nm ultraviolet light in 3 ns pulse widths, with a pulse frequency of 1.5 Hz. Two different reflectron time-of-flight mass spectrometers have been utilized for the detection of the resulting ions. Unless otherwise stated, a combination of linear flight tube and a reflectron has been used in which a curved field for ion reflection was applied (Kratos Kompact MALDI IV, Kratos, Inc., Manchester, UK). This instrument operates a continuous acceleration voltage of 20 kV. The linear flight tube houses a deflection electrode (the ion gate), which allows the selection of ions as a function of their arrival times at the gate and has been utilized here for the detection of ions that undergo delayed ionization. Each individual ToF mass spectrum shown represents the accumulation of 200 single-laser-shot spectra. The resolution was below 1000.

To establish the isotopic pattern of ions above 1000 Da, the coalescence reactions have been performed utilizing a reflectron ToF instrument of higher resolving power (TofSpec 2E, Micromass Ltd., Altrincham, Manchester, UK). Applying the technique of time lag focusing (delayed extraction) with a delay of approximately 550 ns, a sufficient resolution of several thousand could be achieved.

The target compounds have been synthesized according to methods reported in the literature.[12] For the LDI experiments, the samples were deposited on a stainless steel slide as toluene solutions at a 1 mg/mL concentration and dried in an air stream preceding the insertion into the ion source of the mass spectrometer

Results and Discussion

Formation of Azafullerenes. The compounds under investigation are shown in Figure 1. The $(C_{59}N)_2$ dimer **1** is readily obtained in macroscopic quantities from the bisazafulleroid **2**,[12] for which the monoazafulleroid **3** is the synthetic precursor. In the monoazafulleroids, the nitrogen atom links two adjacent carbon atoms of the same five-membered ring by replacing the former C−C σ-bond between them. While in bisadduct **2**, two initially adjacent C−C bonds are bridged by the nitrogen ligands, in compounds **4** and **5** two isolated single bonds of the five-membered ring are substituted by the nitrogen bridges which are now also linked with each other via a trimethylene and a dimethylenoxo bridge, respectively. Compound **6** represents the C_{70} analogue of compound **3**.

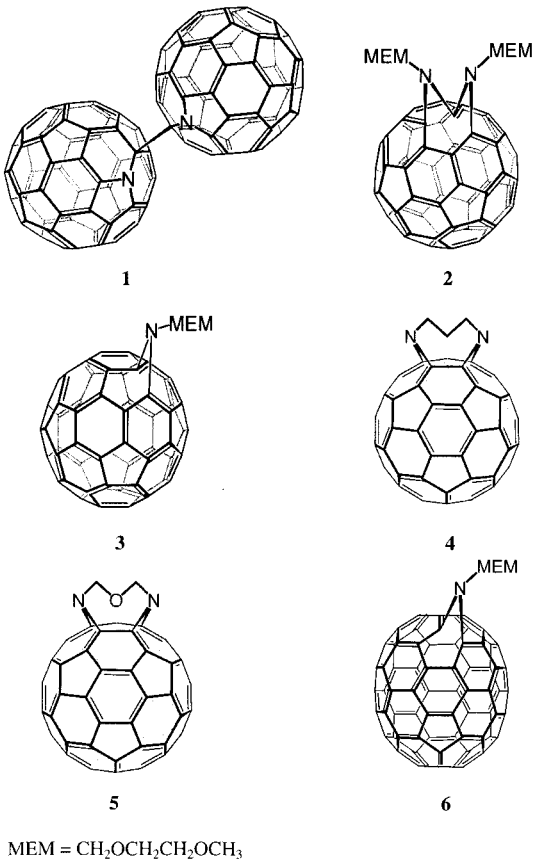

MEM = $CH_2OCH_2CH_2OCH_3$

Figure 1. The structures of the compounds under investigation, see text for details.

Both of the two independently developed syntheses of dimeric $(C_{59}N)_2$ were inspired by mass spectrometry.[11−13] Applying fast atom bombardment (FAB) or liquid secondary ion mass spectrometry (LSIMS) the $C_{59}N^+$ cation was observed from those derivatives which later turned out to be suitable precursors for the macroscopic synthesis.[11−13] In the present study the ligated derivatives **2**−**6** (shown in Figure 1) were also analyzed by LSIMS and $C_{59}N^+$ was found to be produced exclusively from the bisadduct **2**, which is in fact the synthetic precursor for dimeric $(C_{59}N)_2$.

Interestingly, the present direct laser desorption/ionization experiments reveal a strikingly different behavior. The partial positive-ion LDI mass spectra of all ligated azafulleroids are shown in Figure 2 together with the respective region obtained for the $(C_{59}N)_2$ dimer. Besides the expected loss of the attached ligand leading to C_n^+ with $n = 60$ at m/z 720 and $n = 70$ at m/z 840, all compounds undergo an unexpectedly efficient conversion into the $C_{n-1}N^+$ heterofullerene ion with $n = 60$ at m/z 722 or with $n = 70$ at m/z 842. Considering the composition of the attached organic ligand, the ions observed at m/z 722 can in principle be composed of three major isobaric contributions. These are $[^{12}C_{58}{}^{13}C_2]^+$, $[^{12}C_{59}{}^{14}N]^+$, and $[^{12}C_{60}H_2]^+$. The latter ion was shown to produce intact molecular ions under conditions similar to those applied here.[23] Using a Fourier transform ion cyclotron resonance (FTICR) mass spectrometer in conjunction with LDI, we have recently investigated the mono- and bisazafulleroids **3** and **2** with respect to the occurrence of the so-called peak confluence phenomenon.[24] These experiments[25]

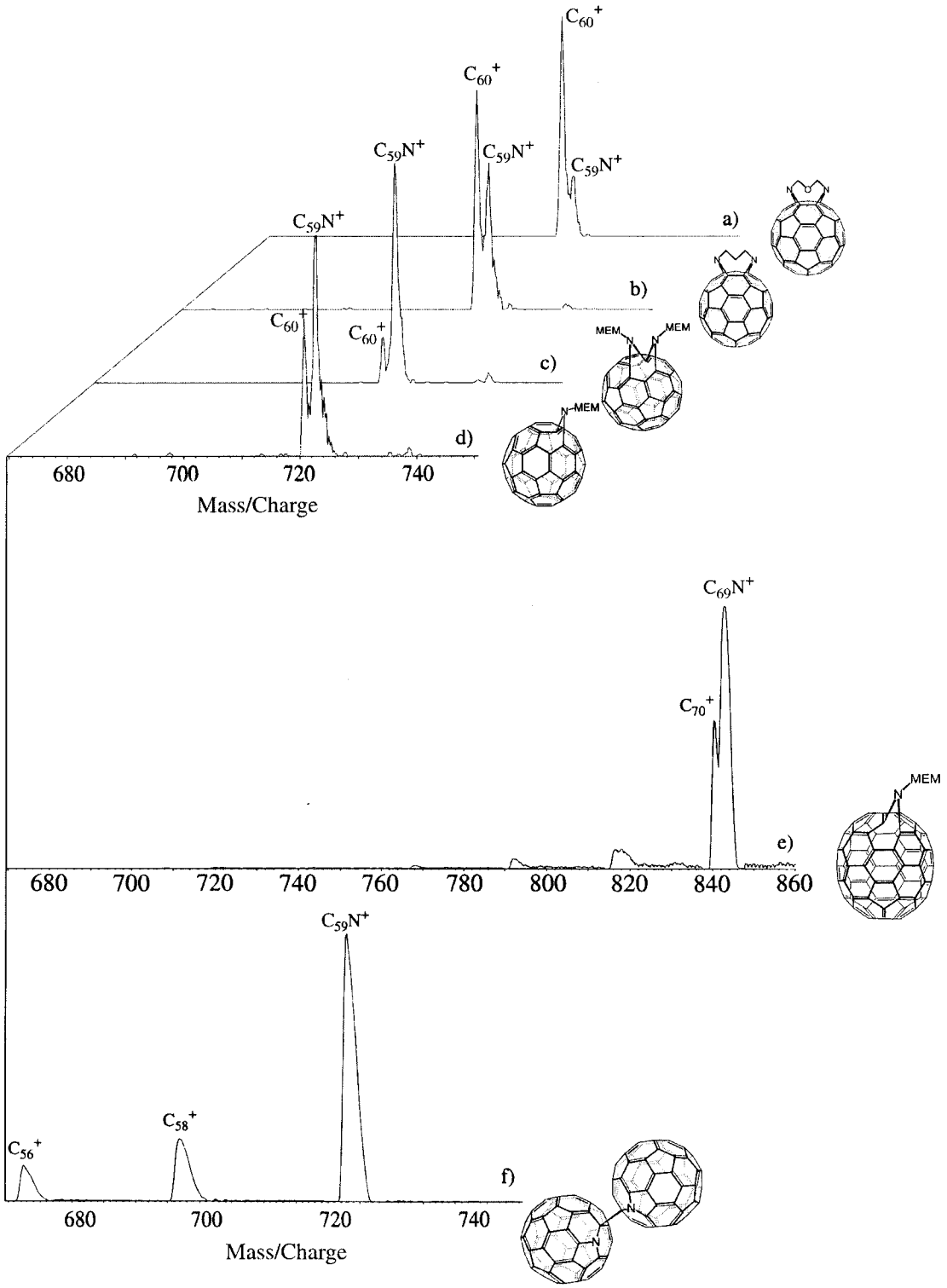

Figure 2. The partial positive-ion laser desorption mass spectra showing the formation of the nitrogen-doped heterofullerene from (a) compound **5**, (b) compound **4**, (c) compound **2**, (d) compound **3**, and (e) compound **6**. Figure 2f shows the dissociations of $C_{59}N^+$ as derived from $(C_{59}N)_2$, proceeding predominately by the loss of CN and followed by the loss of C_2.

were conducted at a mass resolving power which was twice as high as necessary to resolve all possible isobaric ions from each other and it was clearly shown that the signal at *m*/*z* 722 was only composed of $[^{12}C_{59}{}^{14}N]^+$ as the major component with a minor contribution of $[^{12}C_{58}{}^{13}C_2]^+$, while $[^{12}C_{60}H_2]^+$ ions were entirely absent. By analogy, it can be safely assumed that the heterofullerene ions $C_{n-1}N^+$ constitute the major component of the signals observed at *m*/*z* 722 ($n = 60$) and *m*/*z* 842 ($n = 70$).

As can be seen in Figure 2, both C_{60}^+ and $C_{59}N^+$ are efficiently formed from all the ligand-bearing precursors. This is further corroborated by a careful variation of the laser fluence from the threshold value for the formation of ions up to the point at which C_{60}^+ and $C_{59}N^+$ undergo further fragmentation. Compound **5** was found to be the least favored $C_{59}N^+$ precursor, leading to poor quality spectra with $C_{59}N^+$ only clearly detectable at lower laser fluences. The fact that none of the target compounds provided intact molecular ions under the applied conditions makes it difficult to obtain insight into the actual mechanism of the $C_{59}N^+$ formation. Illustrative dissociation experiments of mass selected, potential precursor ions, as

recently so elegantly conducted[8] to elucidate the formation mechanism of networked metallofullerenes, could therefore not be performed.

Even the charge state at which the formation of the heterofullerene might occur initially cannot be assigned unambiguously. Under the applied conditions, neutral C_{60} needs to absorb at least three 337 nm-photons to overcome the ionization threshold. Assuming a similar ionization threshold for organic derivatives of C_{60}, the ionization is achieved by accumulating several energy quanta. This stepwise excitation toward the ionization limit is very likely to induce the efficient liberation of attached ligands already in the neutral state. While ionization followed by dissociation is certainly one major pathway to C_{60}^+, a considerable proportion of the C_{60}^+ ions observed has therefore to be assumed to result from dissociation of the excited neutral molecule followed by electron emission into the cation radical. A similar scenario can in principle be encountered for the formation of $C_{59}N^+$. The formation has to be regarded as a rearrangement involving cage rupture and networking of the heteroatom rather than a simple dissociation reaction.

Interestingly, anionic $C_{59}N^-$ is also effectively formed in the present experiments. $C_{59}N^-$ is a perfectly stable gas-phase ion and readily accessible from the neutral dimer by, for instance, LDI[5] or resonant electron capture[26] (suggesting a positive electron affinity). Laser desorption of the compounds under investigation led to the formation of $C_{59}N^-$ in a similar manner as shown for the cation in Figure 2. The formation of $C_{59}N^-$ could not be readily established only in the case of compound **4**. If this ion was formed, its abundance remained indistinguishable from the expected intensity of $^{12}C_{58}{}^{13}C_2^-$ at *m*/*z* 722. Also, for the formation of neutral $C_{n-1}N\cdot$ distinct differences could be observed. As will be outlined in more detail below, the diazafullerene **2** is the only ligated compound for which $C_{59}N\cdot$ neutrals undergoing delayed ionization could be detected, which in turn provides evidence for the efficient production of the heterofullerene from neutral molecules. Although the nitrogen insertion cannot be directly studied here, these findings show that $C_{59}N$ can be generated in all three charge states examined. Only cationic $C_{59}N^+$ is readily observed for all precursors which probably indicates that the formation process preferentially occurs in this charge state.

Another important mechanistic feature to be addressed here concerns the question of the inter- versus intramolecular nature of the $C_{59}N^+$ formation during the laser ablation process. When performed in a nitrogen atmosphere, both laser ablation[2] and arcing[5,27] of graphite leads to the formation of nitrogen-containing heterofullerenes. Nitrogen atoms can also be networked into nanotubes, when production is carried out in a nitrogen atmosphere,[5] and bombardment of gaseous C_{60} with nitrogen ions also leads to the formation of $C_{59}N^+$.[28] In each of these approaches, conditions are met which allow the inclusion of nitrogen into the carbon framework which is initially free and not attached to the fullerene. The laser ablation of the target compounds could lead to a similar situation in which highly excited nitrogen containing fragments might react with the fullerene core. To elucidate as to whether such processes are of any concern in the present experiments, a mixed target containing pure C_{60} and C_{70}NMEM (compound **6**) in equimolar amounts was laser ablated. The corresponding spectra revealed the efficient formation of C_{60}^+, C_{70}^+ and $C_{69}N^+$ ions, but no indication of any $C_{59}N^+$ formation could be attained. By analogy, the ablation of a mixed target containing pure C_{70}^+ and C_{60}NMEM (compound **3**) gave no indication for the formation of $C_{69}N^+$. Thus, for the conditions applied here, these findings clearly indicate that the $C_{59}N^+$ formation is predominantly of intramolecular nature. As a consequence of this, it is possible to assume a greater influence on the formation of $C_{59}N^+$ caused by the structural features of the nitrogen-containing ligand and the mode of attachment to the fullerene, than is the case for an intermolecular reaction involving only small, energized nitrogen-bearing fragments.

The inclusion of more than one nitrogen atom into the framework has been mentioned previously in the literature[13,27,29] and the formation of $C_{58}N_2^+$ would be, at first sight, a logical consequence for diligated molecules. These could be expected to undergo the formal substitution of a carbon atom by nitrogen twice. Considering the structural features of all the target molecules containing a double nitrogen attachment, it seems plausible to assume that the close proximity by which the two nitrogen atoms are connected to the cage might prevent the double nitrogen incorporation. In all cases the two nitrogen atoms are bound to the same five-membered carbon ring. In compound **2**, the two nitrogen bridges are adjacent and in compounds **4** and **5**, the two nitrogen bridges are spaced by just one C−C bond single bond. $C_{59}N^+$ is generated from all target molecules intramolecularly and the common structural feature is that the nitrogen attachment replaces a C−C single bond connecting a five- and six-membered carbon ring. Assuming that this arrangement might be essential to the laser-induced implementation of nitrogen into the framework, a second ligand attached to the same five-membered carbon ring gives rise to the opening of in total three former isolated rings. Such a structure might not necessarily favor the nitrogen implementation. However, if one of the two ligands is released upon activation, a situation is recreated as with the monoligated species and the heterofullerene formation can take place.

The partial LDI mass spectrum of the $(C_{59}N)_2$ dimer shown in Figure 2 was obtained at a sufficiently high laser fluence to promote fragmentations of the monomeric $C_{59}N^+$ ion. As will be seen in the following discussion, the dissociation behavior of $C_{59}N^+$ adds to the understanding of the coalescence behavior of this heterofullerene. The essential observation has to be seen in the fact that by far the most prominent process is the evaporation of CN from $C_{59}N^+$. This finding is in line with earlier reports applying different means of promoting the fragmentation.[11,13] The first fragment ion signal from $C_{59}N^+$ is spaced by 26 mass units, followed by daughter ion peaks that are separated by 24 mass units formally indicating the preceding loss of C_2 units.

Laser-Induced Coalescence. An interesting phenomenon accompanying the laser ablation process of matter is the ability of the ablated, energized particles to react with each other in the plume of rapidly expanding material into the gas-phase.[14−18] The resulting product distribution can provide important insight into the composition and reactivity of the particles present in the plume. For the ablation of pure fullerene targets, these so-called coalescence reactions lead to the formation of larger carbon clusters. These possess giant fullerene structure rather than dumbbell shape geometry, and their distribution shows enhancements close to multiples of the initial fullerene. This strongly suggests that fullerene coalescence involves the aggregation of moieties which are of very similar size as the ablated target fullerene and that this process is accompanied by C_2 loss fragmentation as well as by C_2 uptake and incorporation into the cage. Enhanced coalescence reactivity could be achieved when ablating certain derivatized fullerenes,[16,30] and efforts were made to gain more control over the product distribution by the use of tailor-made target materials.[16,17,31,32]

Depending on the mode of activation, fullerene oxides can be either coalesced into larger pure carbon clusters[16] or can be fused in soft aggregation reactions into intact dimeric forms,[31,32] which could not be produced by other synthetic approaches.

In this context, it is important to reveal the material properties that might result from doping the carbon cage. Therefore, the laser-induced coalescence reactions of the nitrogen-doped $C_{59}N$ heterofullerene are examined in the following. As an incorporated nitrogen atom is two mass units heavier than carbon, it is possible to use mass spectrometry to determine the involvement of nitrogen in the formation of larger carbon clusters. The coalescence experiments were performed with a higher resolving reflectron-ToF mass spectrometer (see Experimental Section for details), to allow the signals of different nominal masses in the coalescence region to be distinguished.

The positive-ion LDI mass spectrum shown in Figure 3 reveals the efficient formation of clusters in the mass/charge range of approximately 1000−1400 Da. There can be no doubt about the origin of these clusters as being the result of coalescence rather than fragmentations of the dimeric $(C_{59}N)_2$, which is well documented to dissociate, even under gentler conditions than used here, predominantly into $C_{59}N^+$.[12] The analysis of the isotopic pattern obtained for the coalescence signals provides evidence for the cogeneration of pure carbon cluster ions of the type C_n^+, with *n* being an integer number, and of nitrogen-containing species of the formula $C_{n-1}N^+$. The graph in Figure 3 shows the ratio of the nitrogen-doped clusters ($C_{n-1}N^+$) to their pure carbon counterparts ($C_n^{+\cdot}$) and the insert illustrates how these ratios were derived from the experimental data displaying the isotopic pattern obtained for $C_{110}/C_{109}N$ as an example. The height of the signal of lowest mass, which has to be entirely composed of $^{12}C_n^+$, determines the abundance to be expected for $^{12}C_{n-2}{}^{13}C_2^+$ ions which contribute to the intensity of the signal observed two mass units higher. The difference between the measured intensity and the calculated abundance of $^{12}C_{n-2}{}^{13}C_2^+$ must be due to the contribution of $^{12}C_{n-1}N^+$. On the basis of earlier experiments,[25] one can exclude the possibility of hydrogen contaminations which would falsify these considerations. The experimental uncertainty is given as error bars in the diagram in Figure 3. The deviation of calculated and measured abundances was determined by using a pure fullerene target. For coalesced carbon cluster ions the maximum intensity deviation amounts to approximately ±20%. This maximum uncertainty has been deduced from the least abundant coalescence signals and is much lower for abundantly observed coalescence products. In fact, a close match of the expected and measured isotopic pattern was achieved for fullerene ions which originated from neutral precursors already present in the sample. The fact that coalescence reactions take place in the acceleration region of the ion source might have a disturbing effect on the accuracy by which less abundant ions are sampled. As a consequence, the low intensity peaks at the edges of the coalescence envelope derived from the ablation of $(C_{59}N)_2$ were not considered for the diagram in Figure 3. It should be noted, however, that the signals at the high mass end show a clear enhancement of the isotopic peaks that would correspond to $C_{n-2}N_2^+$ ions. Unfortunately, the low abundance in this region prevents an unambiguous confirmation of this assignment. Nevertheless, the cogeneration of pure and one species of nitrogen-containing carbon clusters could be established beyond any doubt. Moreover, Figure 3 shows a clear trend within the coalesced clusters in that the nitrogen-containing clusters dominate the high mass end of the coalescence region while pure carbon clusters are more pronounced at lower masses. The formation of $C_{n-1}N^+$ clusters is in line with the mechanistic ideas derived from earlier investigations of the coalescence of pure fullerenes.[15] It was established that fragmentation of the initial target fullerene is an essential prerequisite for fullerene fusion to occur.[18] By analogy, $C_{59}N$ is the only nitrogen-containing species initially generated by ablation of the corresponding dimer. The smaller fragments are pure carbon clusters, as demonstrated by the laser-induced dissociations of $C_{59}N^+$ (shown in Figure 2f)) which displays predominantly CN loss followed by losses of C_2 units. Therefore, the fusion of $C_{59}N$ with smaller, pure carbon cluster fragments is as likely a scenario for the generation of larger $C_{n-1}N^+$ clusters as the aggregation of two initially intact $C_{59}N$ species accompanied by CN loss and followed by evaporation of C_2 moieties.

The formation of large pure carbon clusters from a heterofullerene target which is entirely free of pure fullerenes seems amazing at first sight. Again, fragmentation accompanying the coalescence process is probably of key importance. However, it seems very unlikely to assume that a considerable amount of those larger, pure carbon-containing products are generated by the fusion of those pure carbon clusters derived from dissociations of the initial $C_{59}N$. The mass spectrum in Figure 3 indicates quite clearly that $C_{59}N^+$ is by far the most prominent species generated from the $(C_{59}N)_2$ dimer and there exists no obvious reason not to assume that also the most prominent neutral ablated would probably correspond to the $C_{59}N^{\cdot}$ radical. Therefore, it is unlikely that the efficient formation of larger C_n^+ clusters, as observed in Figures 3 and 4, results from the fusion of such minor amounts of pure carbon cluster fragments resulting from $C_{59}N^{+/0}$ dissociations. Alternatively, and far more likely, is the assumption that the coalesced $C_{n-1}N^+$ clusters undergo CN loss efficiently, which is probably followed by the loss of C_2 units. This process would have to occur abundantly in the ion source following the initial formation of the $C_{n-1}N^+$ clusters and would provide a reasoning for the rise in abundance of the pure carbon clusters observed at the low mass end of the envelope of coalescence signals (Figure 3 and diagram).

Another strong indication for the assumption that the coalesced pure carbon clusters are formed predominantly via CN loss from $C_{n-1}N^+$ results from the observation of signals due to metastable ion dissociations. Figure 4 allows a more detailed insight into the coalescence region of the positive-ion LDI mass spectrum of the $(C_{59}N)_2$ target. The enlargement of the isotopic pattern obtained for $C_{100}{}^+/C_{99}N^+$ and $C_{102}{}^+/C_{101}N^+$ reveals the appearance of signals between the expected peaks for the stable $C_n^+/C_{n-1}N^+$ ions. The peaks characterized by the asterisks appear at noninteger *m*/*z* values which do not correspond to any mass that can be derived combining carbon and nitrogen and the peaks are slightly broader than those at nominal masses. These features are characteristic for signals derived from ion dissociations occurring after acceleration in the linear flight tube of the instrument. Recently, a general relationship has been derived that connects the *m*/*z* values for the stable parent- and daughter-ion with the one of the metastable fragment ion mass allowing the assignment of the actual metastable.[33] This investigation also provides a thorough evaluation of the uncertainties between the calculated and the experimentally obtained peak position for metastable transitions investigated with the same instrumentation used here. In the present case, a signal arising from metastable C_2 loss from C_n^+ clusters would be spaced by only 0.14 mass units from the corresponding peak for a CN loss from a metastable $C_{n-1}N^+$ precursor. This mass difference, however, is well within the measured deviations that were established for the calculated and the observed *m*/*z* values

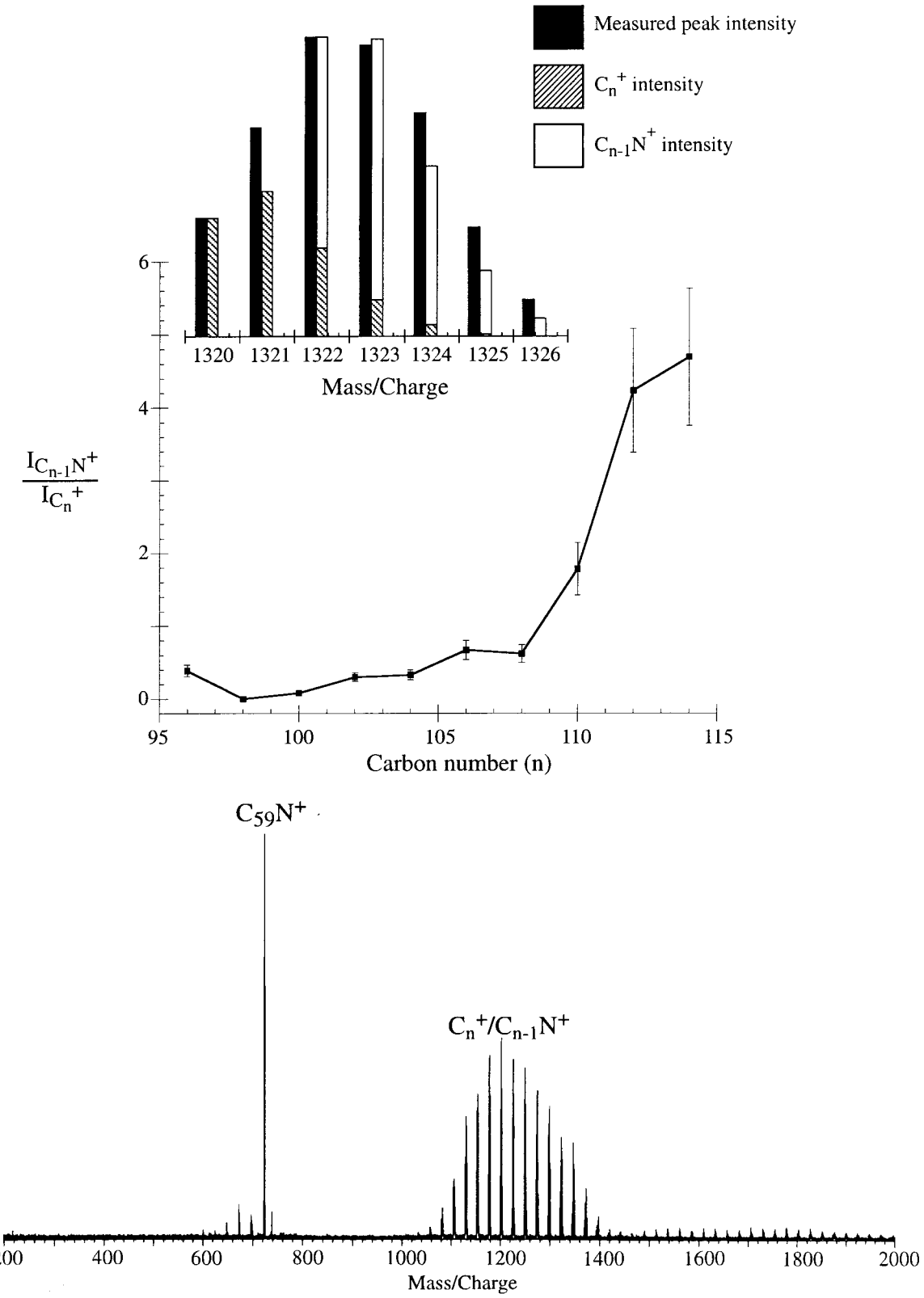

Figure 3. Bottom: The positive-ion laser desorption mass spectrum of $(C_{59}N)_2$, showing $C_{59}N^+$ as the major product ion together with the abundant formation of coalescence products composed of both, C_n^+ and $C_{n-1}N^+$ clusters. Top: The diagram depicts the relative ratio of nitrogen-doped to pure carbon clusters as a function of the cluster size ($n = 96-114$). The insert gives the measured and calculated peak intensities for $C_{110}/C_{109}N$ as an example.

for metastable transition in this mass range. The comparison of the calculated ion peak position with the spectral data would therefore not unambiguously enable the distinction between C_2 and/or CN loss from C_n^+ and/or $C_{n-1}N^+$ parent ions. There is, however, circumstantial support for the CN loss from $C_{n-1}N^+$. When pure C_{60} is coalesced under identical conditions, the signals for metastable dissociations are entirely absent. Thus, under the present conditions, C_2 losses from large C_n^+ clusters are practically not detectable in the LDI mass spectrum. On the basis of this finding, together with the assumption that the

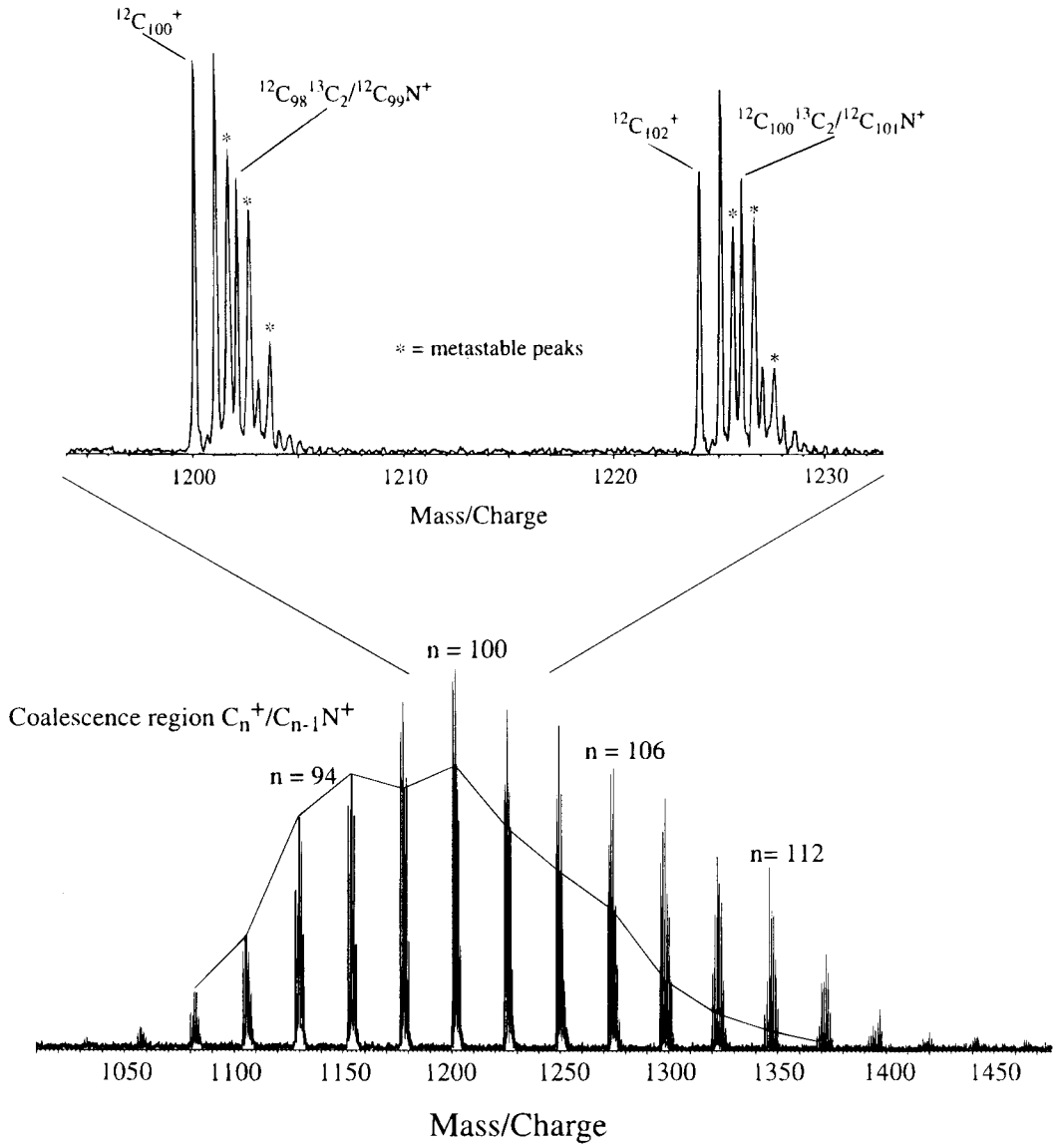

Figure 4. Bottom: The enlargement of the coalescence region derived from positive-ion laser desorption of $(C_{59}N)_2$. The lines connect the highest peaks observed in each set of signals that result from metastable decay. Top: Enlarged display of the signals observed for $C_{100}^+/C_{99}N^+$ and $C_{102}^+/C_{101}N^+$. The signals arising from metastable decay are clearly resolved and characterized by asterisks. See text for details.

large C_n^+ clusters generated from $(C_{59}N)_2$ possess the same structural features as those generated from C_{60} (i.e., possess giant fullerene structures), the possibility that the observed metastable peaks correspond to C_2 loss from pure carbon clusters can be discounted. In contrast to the lack of metastable signals from coalescence products of C_{60}, the coalescence signals derived from mono- and diazafullerenes **2** and **3** (Figure 1) show a similar appearance of metastable transition signals as observed from the ablation of $(C_{59}N)_2$. As both these precursors produce $C_{59}N$ efficiently, which subsequently undergoes coalescence reactions to generate larger $C_{n-1}N^+$ clusters, this strongly indicates that the observed metastable transitions are intrinsically connected with dissociations proceeding from the larger, coalesced $C_{n-1}N^+$ clusters. As the laser-induced fragmentation of $C_{59}N^+$ commences by the predominant CN loss, one can probably assume an analogous fragmentation dynamic for larger nitrogen-containing heterofullerenes, so that it seems fairly plausible to assign the observed metastable transition signals to the dissociation of $C_{n-1}N^+$ clusters into C_{n-2}^+ via the loss of CN. Finally, no evidence was found for metastable decay leading to similarly sized neutrals and charged fragments. This confirms the structural assignment of the large $C_{n-1}N^+$ clusters as giant heterofullerenes rather than dumbbell-like aggregates for which a fission into the two components (i.e., the initial $C_{59}N$ moiety and a pure C_n entity) would most likely compete with the observed CN loss.

Delayed Ionization. One of the most remarkable characteristics of fullerenes is their ability to undergo ionization after a delay, following the excitation event. The phenomenon of delayed electron emission was first observed in laser desorption/laser ionization experiments[19,20] and followed by numerous investigations which were aimed at obtaining an understanding of the ionization dynamics involved.[21] While there exist several explanations of the actual mechanism, it was found that delayed ionization can be induced by a variety of ionization methods and the experimental parameters influencing the process could be established. The kinetics of delayed ionization depend on the nature of the fullerene and the mode of excitation.[15] Only in cases where the excitation energy cannot be released sufficiently via fragmentation pathways has it been possible to observe delayed ionization. Fullerene derivatives, for instance, can readily release the attached ligands upon excitation, so that in these cases delayed electron emission has been observed only from the bare carbon core and not from the intact derivative.[17,22]

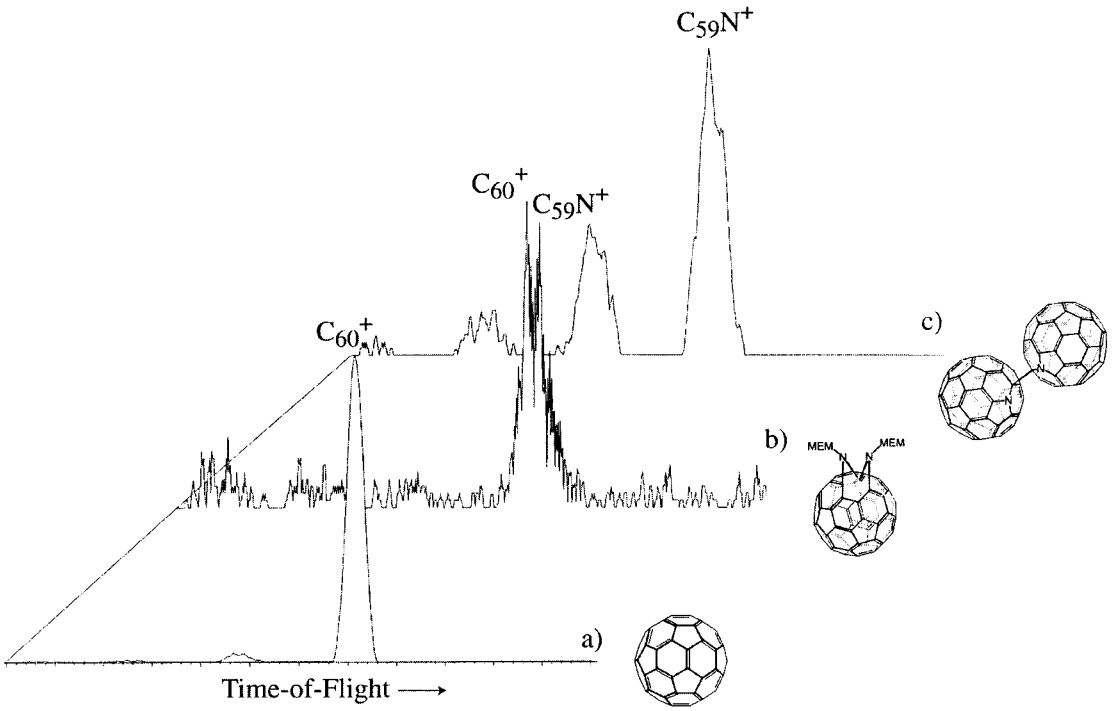

Figure 5. Positive-ion laser desorption/ionization mass spectra obtained by using an ion gate to deflect all prompt ionizing ions below *m*/*z* 1000 and above *m*/*z* 1005. The spectra display the signals arising from delayed ionization of (a) C_{60}, (b) C_{60}, and $C_{59}N^{\cdot}$ from compound **2**, and (c) $C_{59}N^{\cdot}$ from compound **1**. The allowed time window corresponds to a delay in ionization of approximately 0.5 μs.

In turn, the observation of delayed ionization of fullerenes can be regarded as a sign of remarkable stability toward fragmentation, imposing on the comparison with their nitrogen-doped counterparts.

In the following, LDI experiments are discussed in which ions resulting from delayed electron emission are sampled. Applying a continuous acceleration voltage in conjunction with an ion gate for flight time-resolved ion selection, it was recently noted that the dissociation spectra (commonly referred to as Post Source Decay (PSD) spectra) of mass selected fullerenes can be tremendously interfered with by signals resulting from delayed ionizing target molecules.[34] This observation can in turn be used to study delayed ionization. The principle of the experiment is detailed below. Molecules are desorbed and ionized by a laser pulse and extracted by a static electric field into a flight tube which uses an ion gate for the selection of ions. The ion gate consists of two deflecting electrodes which are switched off for a short period of time at the arrival time of the ions of interest allowing only them to pass. If the ion path then leads through a reflectron, the selected ion and possible fragment ions thereof are energetically resolved leading to a PSD spectrum. The molecular ion of the target compound is the slowest of all the ions generated in a prompt ionization event (we do not consider coalescence and aggregation phenomena at this point) and therefore it needs the longest time to reach the ion gate. If the ion gate is however set to select a species of larger mass than present in the sample material, only ions that require an even longer time to reach the ion gate than the largest (and thus slowest) ion resulting from prompt ionization are sampled. Ions caused by delayed ionization possess an extended flight time due to the longer residence of the corresponding neutral in the source. The ion gate is thus used to select a nominal mass greater than the parent ion, though no such ions exist. Any signals detected arise from delayed ions alone passing the ion gate. Therefore, this experiment reveals species which underwent delayed ionization.

In Figure 5 the spectra obtained from such experiments are depicted for the ablation of C_{60} (Figure 5a), the bisadduct **2** ($C_{60}(NMEM)_2$, Figure 5b) and the dimer **1** (($C_{59}N)_2$, Figure 5c), respectively. In these experiments, the ion gate is set to select a mass region which corresponds to a delay time in ionization of approximately 0.5 μs. As the resolving power and the mass accuracy are lower than in the normal operating mode, C_{60} (Figure 5a) is used for calibration, i.e., to indicate the position at which the delayed ion signal for *m*/*z* 720 is detected. The $(C_{59}N)_2$ dimer sample was entirely free of any trace of C_{60} to prevent artifact signals arising from it. This leaves no doubt that the signal observed in Figure 5c is caused by delayed ionization of $C_{59}N^{\cdot}$. For the diazafullerene, compound **2**, two signals were obtained corresponding to the delayed ionization of C_{60} and $C_{59}N^{\cdot}$. The fact that $C_{59}N^+$ is observed as the result of delayed electron emission from $C_{59}N^{\cdot}$, which in turn was generated from a derivative in which the nitrogen is attached exohedrally, shows that the networking of the nitrogen atom can also take place in the neutral state. Unfortunately, more detailed insight into the kinetics of the delayed electron emission from $C_{59}N^{\cdot}$ could not be achieved at present. When recorded as a function of the delay time, the abundance of the $C_{59}N^+$ ions was found to be too strongly affected by inhomogeneties in the $(C_{59}N)_2$ target layer, in that the ion abundance varied too strongly to allow quantitative insight. While efforts are currently underway to improve the homogeneity of the $(C_{59}N)_2$ film, the present data clearly show that the $C_{59}N^{\cdot}$ heterofullerene undergoes delayed electron emission, which indicates a similar resistance toward fragmentation as is found in their pure-carbon counterparts.

Conclusion

Nitrogen atoms initially attached to fullerenes in an exohedral fashion have been efficiently implemented into the carbon network of fullerenes by applying laser desorption/ionization. The abundant formation of both cationic and anionic $C_{n-1}N^{+/-}$

heterofullerenes where $n = 60$ or 70 has been observed. Evidence has been presented for the intramolecular nature of $C_{59}N^+$ formation. A common feature of the investigated target molecules is the location of the nitrogen bridge at a C−C bond shared by one five- and one six-membered carbon ring. This new method of modifying the fullerene cage might therefore be potentially of relevance to the selective modification of the endcaps of all-carbon nanotubes, representing the location of five-membered rings in the tube.

The laser ablation of $(C_{59}N)_2$ is accompanied by coalescence reactions leading to both larger pure C_n^+ (n = even) and $C_{n-1}N^+$ clusters. The formation of both these clusters are most probably caused by fusion reactions involving the initially formed $C_{59}N$ fragments. The pure carbon clusters are most likely formed by CN loss from larger $C_{n-1}N^+$ ions, as supported by the observation of the corresponding metastable transitions.

The nitrogen heterofullerenes are shown to undergo delayed ionization, the first observation of this phenomenon for doped fullerenes. This finding implies a similar stability and resistance toward fragmentation as found for pure fullerenes, otherwise the delayed electron emission process could not compete with the energy release via dissociation channels.

Acknowledgment. The authors are thankful to Prof. P. J. Derrick for machine time at the National FT-ICR Facility at Warwick which led to the confirmation of the heterofullerene identity by high resolution/high mass accuracy mass spectrometry. It is a pleasure to acknowledge Dr. G. Critchley and Dr. D. Gostick of Micromass Ltd., Altricham, UK, for providing access to the high resolving Tof-Spec 2E instrument. We are indebted to The Leverhulme Trust and the EPSRC for the financial support of the work performed at Warwick.

References and Notes

(1) Guo, T.; Jin, C.; Smalley, R. E. *J. Phys. Chem.* **1991**, *95*, 4948−4950.

(2) Ying, Z. C.; Hettich, R. L.; Compton, R. N.; Haufler, R. E. *J. Phys. B: At. Mol. Opt. Phys.* **1996**, *29*, 4935−4942.

(3) Kimura, T.; Sugai, T.; Shinohara, H. *Chem. Phys. Lett.* **1996**, *256*, 269−273.

(4) Pellarin, M.; Ray, C.; Mélinon, P.; Lermé, J.; Vialle, J. L.; Kéghélian, P.; Perez, A.; Broyer, M. *Chem. Phys. Lett.* **1997**, *277*, 96−104.

(5) Yu, R.; Zhan, M.; Cheng, D.; Yang, S.; Liu, Z.; Zheng, L. *J. Phys. Chem.* **1995**, *99*, 1818−1819.

(6) Muhr, H.-J.; Nesper, R.; Schnyder, B.; Kötz, R. *Chem. Phys. Lett.* **1996**, *249*, 399−405.

(7) Möschel, C.; Jansen, M. *Z. Anorg. Allg. Chem.* **1999**, *625*, 175−177.

(8) Branz, W.; Billas, I. M. L.; Malinowski, N.; Tast, F.; Heinebrodt, M.; Martin, T. P. *J. Chem. Phys.* **1998**, *109*, 3425.

(9) Poblet, J. M.; Muñoz, J.; Winkler, K.; Cancilla, M.; Hayashi, A.; Lebrilla, C. B.; Balch, A. L. *Chem. Commun.* **1999**, 493−494.

(10) Kimura, T.; Sugai, T.; Shinohara, H. *Int. J. Mass Spectrom.* **1999**, *188*, 225−232.

(11) Hummelen, J. C.; Knight, B.; Pavlovich, J.; González, R.; Wudl, F. *Science* **1995**, *269*, 1554.

(12) Nuber, B.; Hirsch, A. *Chem. Commun.* **1996**, 1421.

(13) Lamparth, I.; Nuber, B.; Schick, G.; Skiebe, A.; Grösser, T.; Hirsch, A. *Angew. Chem., Int. Ed. Engl.* **1995**, *34*, 2257.

(14) Yeretzian, C.; Hansen, K.; Diederich, F.; Whetten, R. L. *Nature* **1992**, *359*, 44.

(15) Beck, R. D.; Weis, P.; Bräuchle, G.; Kappes, M. M. *J. Chem. Phys.* **1994**, *100*, 262.

(16) Beck, R. D.; Stoermer, C.; Schulz, C.; Michel, R.; Weis, P.; Bräuchle, G.; Kappes, M. M. *J. Chem. Phys.* **1994**, *101*, 3243.

(17) Beck, R. D.; Weis, P.; Hirsch, A.; Lamparth, I. *J. Phys. Chem.* **1994**, *98*, 9683.

(18) Mitzner, R.; Winter, B.; Kusch, C.; Campbell, E. E. B.; Hertel, I. V. *Z. Phys. D* **1996**, *37*, 89.

(19) Campbell, E. E. B.; Ulmer, G.; Hertel, I. V. *Phys. Rev. Lett.* **1991**, *67*, 1986.

(20) Wurz, P.; Lykke, K. R. *J. Chem. Phys.* **1991**, *95*, 7008.

(21) Deng, R.; Echt, O. *J. Phys. Chem. A* **1998**, *102*, 2533−2539.

(22) Beck, R. D.; Weis, P.; Rockenberger, J.; Kappes, M. M. *Surf. Rev. Lett.* **1996**, *3*, 771.

(23) Mandrus, D.; Kele, M.; Hettich, R. L.; Guiochon, G.; Sales, B. C.; Boatner, L. A. *J. Phys. Chem. B* **1997**, *101*, 123.

(24) Mitchell, D. W.; Smith, R. D. *Phys. Rev. E* **1995**, *52*, 4366.

(25) Feng, X.; Clipston, N.; Brown, T.; Cooper, H.; Reuther, U.; Hirsch, A.; Derrick, P. J.; Drewello, T. *Rapid Commun. Mass Spectrom.* **2000**, *14*, 368−370.

(26) Vasil′ev, Y.; et al. **2000**. In preparation.

(27) Pradeep, T.; Vijayakrishnan, V.; Santra, A. K.; Rao, C. N. R. *J. Phys. Chem.* **1991**, *95*, 10564−10565.

(28) Christian, J. F.; Wan, Z.; Anderson, S. L. *J. Phys. Chem.* **1992**, *96*, 10597−10600.

(29) Tobe, Y.; Nakanishi, H.; Sonoda, M.; Wakabayashi, T.; Achiba, Y. *Chem. Commun.* **1999**, 1625−1626.

(30) Ong, P. P.; Zhu, L.; Zhao, L.; Zhang, J.; Wang, S.; Li, Y.; Cai, R.; Huang, Z. *Int. J. Mass Spectrom.* **1997**, *163*, 19−28.

(31) Barrow, M. P.; Tower, N. J.; Taylor, R.; Drewello, T. *Chem. Phys. Lett.* **1998**, *293*, 302−308.

(32) Al-Jafari, M. S.; Barrow, M. P.; Taylor, R.; Drewello, T. *Int. J. Mass Spectrom.* **1999**, *184*, L1 − L4.

(33) Harvey, D. J.; Hunter, A. P.; Bateman, R. H.; Brown, J.; Critchley, G. *Int. J. Mass Spectrom.* **1999**, *188*, 131−146.

(34) Barrow, M. P.; Drewello, T. *Int. J. Mass Spectrom.* In press.